Self-consistent calculation of resonant tunneling in asymmetric double barriers in a magnetic field

P. Orellana
Departamento de Física, Universidad de Santiago, Casilla 307, Correo 2, Santiago, Chile

F. Claro
Facultad de Física, Pontificia Universidad Católica de Chile, Vicuña Mackenna 4860, Casilla 306, Santiago 22, Chile

E. Anda and S. Makler
Instituto de Física, Universidad Federal Fluminense, Avenida General Milton Tavares s/n, Gragoata, 2421-340 Niteroi, Rio de Janeiro, Brazil

(Received 8 September 1995)

We have studied resonant tunneling through an asymmetric double barrier in the presence of a magnetic field in the direction of the current flow. The electron-electron interaction as well as coupling to a longitudinal-optical phonon field are included. The main resonance peak in the *I-V* characteristic is followed by a phonon-induced peak, both showing a structure at finite magnetic field. We find a bistable region whose width oscillates with magnetic field, in accordance with experiment. This region is expected in the main resonance, yet, as we show, it may also be present in the phonon peak in the limit of large asymmetry.

I. INTRODUCTION

Since the seminal work of Tsu and Esaki, double-barrier resonant tunneling structures (DBRTS) have been the subject of much interest for their physical properties and applications as electronic devices.[1] After some of the more basic aspects of charge transport in DBRTS were addressed both theoretically and experimentally, other phenomena associated with such tunneling phenomena have attracted attention. One example is the intrinsic bistability caused by the space-charge formation in the well. The space charge alters the way in which the voltage drop is distributed across the device, which in turn modifies the tunneling current, allowing for the existence of two different states of the system in some range of bias.[2,3]

Other important issues in the study of electron tunneling in nanostructures is the inelastic scattering through the electron-phonon interaction. Goldman, Tsui, and Cunningham provided experimental evidence that the longitudinal-optical phonon assists in tunneling in the valley current region of a DBRTS.[4] There have been several theoretical studies of this problem.[5–7] Also, in recent years there has been an increased interest in magnetotunneling studies in DBRTS with the magnetic field parallel or perpendicular to the current flow.[3,8–11] Magnetotunneling experiments in a parallel magnetic field have been reported by many authors and have provided useful information. In the resonant regime, weak oscillations are observed in the current versus magnetic field curves from which it is possible to deduce the charge buildup in the well and the effective dimensionality of the emitter.[12] In the off-resonance regime, the analysis of the valley current magneto-oscillations provides a very good determination of the different scattering mechanisms contributing to this current.[8] Translational invariance in the plane of the layers implies conservation of Landau-level index for coherent tunneling from the emitter into the well. Breakdown of this selection rule is only observed in the valley current and is due to incoherent elastic- or inelastic-scattering processes. Also, Leadbeater and Eaves reported the observation of an enhancement in the intrinsic bistability region of the *I-V* curve.[9]

In this paper we study the steady-state solutions of the DBRTS in the presence of a magnetic field parallel to the direction of current flow. In our treatment we include electron-electron interactions and the coupling of electrons and phonons in the space between the barriers. We allow the collector barrier width to vary in order to assess the enhancement of both interaction processes, as more charge is trapped in such space. In Sec. II we describe our model and derive the general expressions needed to calculate the charge density along the sample, and the current. In Sec. III a self-consistent numerical procedure is defined and in Sec. IV it is applied to a specific sample. Our conclusions are presented in the summary in Sec. V.

II. THE MODEL

We consider the transport properties of a double-barrier heterostructure in the presence of a longitudinal magnetic field. A tight-binding model is used for the electron Hamiltonian, and coupling to longitudinal-optical (LO) phonons is included within the Fröhlich formalism. The response of the system is studied, introducing a fully self-consistent scheme to treat the electron-electron interaction in the steady state when the bias is applied. Inclusion of a longitudinal magnetic field B (in the growth direction, henceforth called the z direction) is simple if a parabolic energy dispersion parallel to the interfaces is assumed. The field quantizes the motion

0163-1829/96/53(19)/12967(6)/$10.00

of the electrons in the xy plane, giving rise to Landau levels with energies $\epsilon_N=(N+1/2)\hbar\omega_c$, where $N=0,1,2,\ldots$ is the Landau index and $\omega_c=eB/m^*c$ is the cyclotron frequency. Assuming that the longitudinal degree of freedom is decoupled from the transverse motion and that a simple optical phonon mode of frequency ω_0 is relevant the Hamiltonian takes the form

$$H=\sum_l (\epsilon_l+\epsilon_N)c_l^\dagger c_l+t\sum_{\langle ll'\rangle} c_l^\dagger c_{l'}+\hbar\omega_0 b^\dagger b$$
$$+g\sum_l c_l^\dagger c_l(b^\dagger+b)+\frac{U}{2}\sum_{ll'} c_l^\dagger c_{l'} c_l^\dagger c_{l'}, \qquad (1)$$

where the operator $c_l^\dagger$ creates an electron at site l, $b^\dagger$ creates a phonon, t is the hopping matrix element between nearest neighbors $\langle ll'\rangle$, ϵ_l the site energy, and U and g the electron-electron and the electron-phonon coupling constants, respectively. For simplicity we have restricted the Coulomb interaction to the intrasite contribution and we ignored the spin degree of freedom.

The eigenstate may be expanded in an orthonormal basis of localized states of the noninteracting system $|l,n\rangle$,

$$|\psi\rangle=\sum_{l,n} a_l^n|l,n\rangle, \qquad (2)$$

where l is the site of localization and n the number of phonons. Here

$$a_l^n=\langle l,n|\psi\rangle=\frac{1}{\sqrt{n!}}\langle 0|\Theta_l^n|\psi\rangle, \qquad (3)$$

with $|0\rangle$ the vacuum and $\Theta_l^n=c_l^\dagger b^n$. Introducing these latter operators in (1) we find they obey the equation of motion

$$i\hbar\frac{d\Theta_l^n}{d\tau}=(\epsilon_l+n\hbar\omega_0+\epsilon_N)\Theta_l^n+t(\Theta_{l-1}^n+\Theta_{l+1}^n)$$
$$+g\Theta_l^n(b^\dagger+b)+ng\sum_{l'} n_{l'}\Theta_l^{n-1}+U\langle n_l\rangle_n\Theta_l^n, \qquad (4)$$

where $n_{l'}=c_{l'}^\dagger c_{l'}$ and $\langle n_l\rangle_n=\Sigma_\beta|a_l^n(\beta)|^2$, the sum over β covering all occupied electron states in the system.

We have used a mean-field approximation (Hartree) to treat the electron-electron interaction. From Eqs. (2)–(4) we get for the coefficients of a stationary state of frequency ω the equation

$$\epsilon a_l^n=(\epsilon_l+n\hbar\omega_0+\epsilon_N)a_l^n+t(a_{l-1}^n+a_{l+1}^n-2a_l^n)$$
$$+g(\sqrt{n+1}a_l^{n+1}+\sqrt{n}a_l^n)+\frac{U}{2}\sum_\beta |a_l^n(\beta)|^2 a_l^n, \qquad (5)$$

where the energy ϵ is measured from the bottom of the band. This is a nonlinear difference equation for the coefficients a_l^n, its nonlinear character arising from the last term in the right-hand side. The equation of motion for the charge operators $Q_l=ec_l^\dagger c_l$ gives for the current operator at site l, $J_l=dQ_l/d\tau=(et/i\hbar)(c_l^\dagger c_{l+1}-c_{l+1}^\dagger c_l)$. Taking the expectation value of this equation we obtain for the contribution of a state of energy ϵ to the average current,

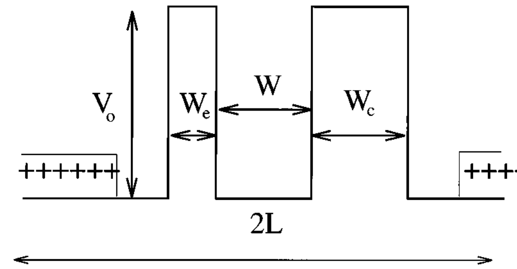

FIG. 1. Built-in potential profile and positive background charge of the device.

$$j_l=\frac{et}{i\hbar}\sum_n (a_l^{*n}a_{l+1}^n-a_{l+1}^{*n}a_l^n). \qquad (6)$$

The total current is calculated integrating this expression over all available states with energy below the Fermi energy.

III. SELF-CONSISTENT LOOP

As is known, the electron-electron interaction in a double-barrier system is responsible for the formation of an accumulation layer at the emitter interface, and a charge buildup between the barriers during resonant tunneling. The latter may cause hysteresis in the I-V curve.[4] In our calculations we include the electron-electron interaction in a region of length $2Ld$, where d is the lattice constant. In this region the charge fluctuations are expected to be important, while outside the electrons effectively behave as free particles. Away from this region we set $U=0$. Also, as the emission of phonons is more likely between the barriers where the electrons spend a long time under resonant conditions, we will take $g\neq 0$ there only. Figure 1 shows the built-in potential profile of the device and the geometry and notation we use.

We first consider the region $z_l<-Ld$. Since $U=g=0$ in this region the solutions to Eq. (5) are just planes waves,

$$a_l^n=I_n e^{ik_n z_l}+R_n e^{-ik_n z_l}, \quad z_l<-Ld, \qquad (7)$$

where k_n is defined by the relation

$$\epsilon=n\hbar\omega_0+\epsilon_N+2t(\cos k_n d-1), \qquad (8)$$

with $t<0$. Notice that we have chosen the origin of energy so that $\epsilon_l=0$ in this region. For k_n real the first and second terms in Eq. (7) represent an incident and a reflected wave of amplitudes I_n and R_n, respectively. The last term in Eq. (8) represents the kinetic energy. For n greater than some $n_0(\epsilon,B)$ this energy becomes negative. This means that $k_n=i\kappa_n$ and the general solution takes the form

$$a_l^n=I_n e^{-\kappa_n z_l}+R_n e^{\kappa_n z_l}, \quad z_l<-Ld. \qquad (9)$$

In order to assure a regular behavior for $z\to-\infty$ the amplitudes I_n have to be set equal to zero for theses modes. They are vanishing modes at the left. On the other hand, for $z_l > Ld$ we have $\epsilon_l = -V$, where V is the applied bias, and the solutions have the form

$$a_l^n = T_n e^{ik'_n z_l}, \quad z_l > Ld, \tag{10}$$

with k'_n defined by

$$\epsilon = -V + n\hbar\omega_0 + \epsilon_N + 2t(\cos k'_n d - 1). \tag{11}$$

Knowing the form of the right ($z_l > Ld$) and left ($z_l < -Ld$) asymptotic solutions the problem is reduced to making them compatible, which is done by iterating numerically Eq. (5) in its slightly rearranged form:

$$\begin{aligned} a_{l-1}^n &= \frac{(\epsilon + 2t - \epsilon_l - \epsilon_N - n\hbar\omega_0)}{t} a_l^n \\ &\quad - \frac{g}{t}(\sqrt{n+1}a_l^{n+1} + \sqrt{n}a_l^n) \\ &\quad - \frac{U}{t}\sum_\beta |a_l^n(\beta)|^2 a_l^n - a_{l+1}^n. \end{aligned} \tag{12}$$

The iteration is performed from right to left by choosing arbitrary values for the coefficients T_n. Applying Eq. (12) until the end point ($z_{-L} = -Ld$) is reached we then obtain the incident and reflected amplitudes by comparing the amplitudes given by the iteration at the two last points with Eq. (7).

In general both the transmission and reflection coefficients are linear functions of the amplitude of incidence. This is expressed by the relations

$$T_n = \sum_m M_{nm}^T I_m,$$

$$R_n = \sum_m M_{nm}^R I_m, \tag{13}$$

or

$$\mathbf{T} = \mathbf{M_T} I,$$

$$\mathbf{R} = \mathbf{M_R} I. \tag{14}$$

Since we start from the right we have to express **I** and **R** as a function of **T**,

$$\mathbf{I} = \mathbf{M_T}^{-1} T,$$

$$\mathbf{R} = \mathbf{M_R} M_T^{-1} T. \tag{15}$$

These relations are convenient in our scheme of computation since they give the reflected and transmitted amplitudes for each choice of the T_n. We now have to determine the matrices M_T and M_R. For simplicity we begin the iteration choosing $T_0 = 1$ and $T_n = 0$, $n = 1,2,\ldots$. With these initial values we get

$$(M_T^{-1})_{n0} = I_n^0,$$

$$(M_R M_T^{-1})_{n0} = R_n^0, \tag{16}$$

where the superscript means that the coefficients were obtained making $T_0 = 1$. We next make $T_1 = 1$ and $T_n = 0$ for $n = 0,2,3,4,\ldots$ and get

$$(M_T^{-1})_{n1} = I_n^1,$$

$$(M_R M_T^{-1})_{n1} = R_n^1. \tag{17}$$

The procedure is repeated up to $n = n_{\max}$, where $n_{\max}$ is the number of channels available in the system. In this way we can calculate all matrix elements, $(M_T^{-1})_{nm}$ and $(M_R M_T^{-1})_{nm}$, from which we can in turn get the matrices M_T and M_R. This allows us to obtain the physical amplitudes T_n and R_n using Eq. (13). We are interested in the low carrier density limit, for which $\epsilon_f < \hbar\omega_0$. In such a case the physical running waves correspond to $I_0 = 1$ and $I_n = 0$, $n = 1,2,\ldots$ so we have

$$T_n = (M_T)_{n0},$$

$$R_n = (M_R)_{n0}. \tag{18}$$

Once the transmission amplitudes T_n are obtained self-consistently we may calculate the current j_l in the collector region. From Eqs. (6) and (10) we have

$$j_l = \frac{2et}{\hbar}\sum_n \sin(k'_n d)|T_n|^2. \tag{19}$$

Summing over all occupied states one gets for the total current the expression

$$J_B = \frac{etV}{2\hbar(\pi l_m)^2}\sum_{N,n}\int_0^{k_{Nf}} \sin(k'd)|T_n(k')|^2 dk, \tag{20}$$

where $l_m = (\hbar c/eB)^{1/2}$ is the magnetic length and V is the volume of the sample.

IV. RESULTS

In this section we show numerical results for the I-V characteristics of an asymmetric DBRTS in the presence of a longitudinal magnetic field. We have chosen a GaAs/$Al_xGa_{1-x}As$ structure at 0 K, with a fixed emitter thickness of $W_e = 1.12$ nm, a variable collector thickness W_c, and a well thickness of 11.2 nm. The conduction-band offset is set at $V_0 = 300$ meV. The system is uniformly doped up to 3.36 nm from either barrier, with a density of ionized donors of 2×10^{17} cm^{-3}. In equilibrium and at zero magnetic field the Fermi level lies 19.2 meV above the asymptotic conduction-band edge. The electron potential due to the applied bias is taken into account through a linear dependence of ϵ_l with l, which is assumed to arise from fixed external charges. This site energy includes the potential due to the barriers. The total potential profile seen by the electron is

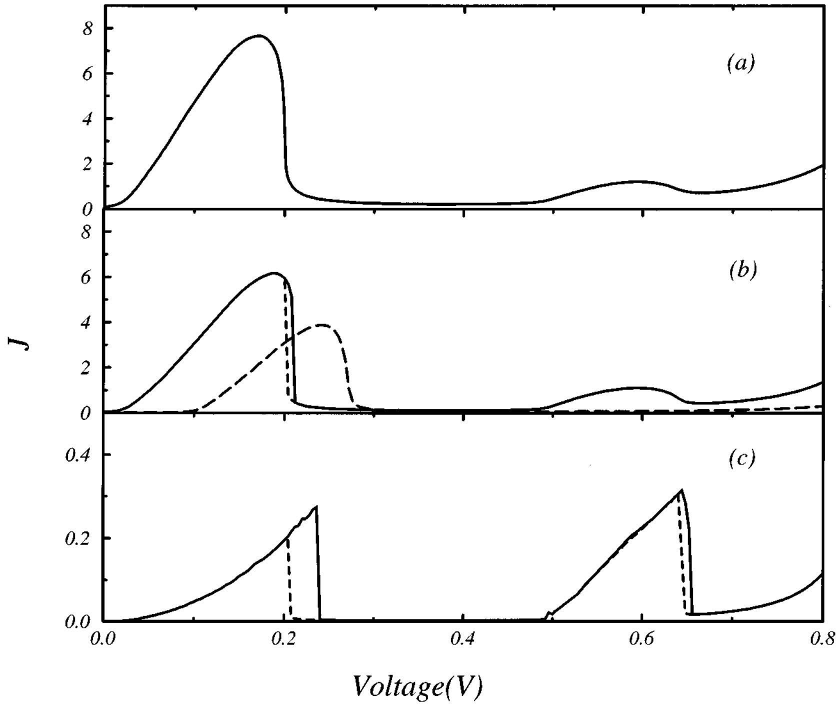

FIG. 2. Current-voltage characteristics at 0 T for (a) $W_c = W_e$, (b) $W_c = 2.5W_e$, and (c) $W_c = 10W_e$. Dashed lines are for decreasing bias. Long-dashed line in (b) is the free-electron approximation.

calculated self-consistently adding to the fixed values of ϵ_l the nonlinear Hartree term appearing in Eq. (5). For the hopping constant in Eq. (12) we use the approximation $t = \hbar^2/2m^*d^2$, which for GaAs has the value $t = 2.16$ eV and $U = 10$ meV. For the LO phonon frequency we take the bulk GaAs value $\hbar\omega_0 = 36$ meV, and for the strength of the electron-phonon interaction, $g = 20$ meV (Ref. 13). In our computations we normalize the self-consistent solutions so as to neutralize the fixed positive charge background of the ionized donors at edges $z_{\pm L} = \pm Ld$.

Figure 2 shows our self-consistent results for the I-V curve at zero magnetic field and different collector barrier thicknesses. Solid (dashed) lines are for increasing (decreasing) bias. There are two peaks, the highest one due to transport with no emission of phonons, while the second peak involves the emission of one phonon. In Fig. 2(a) the barriers have equal thicknesses, while in Figs. 2(b) and 2(c) $W_c = 2.5W_e$ and $10W_e$, respectively. Hysteresis is clearly seen in the asymmetric cases and is absent in the symmetric case. We find that the width of the bistable region increases as the above ratio increases, and saturates at about $W_c = 5.88W_e$. Also, while the phonon peak remains basically unchanged in this process, the height of the first peak is reduced since transmission in this single channel is less probable with a wider collector barrier. Note the different scales in the vertical axis. In the limit of strong asymmetry, hysteresis is present in the phonon peak as well. Turning off the electron-electron and electron-phonon interactions has the effect of eliminating the bistable region as well as the phonon peak, as shown by the long-dashed curve in Fig. 2(b). It is important to mention that the resonant peak appears higher in energy when the many body effects are neglected [long dashed curve in Fig. 2(b)], than in the case where the e-e and e-ph interactions are taken into account. Although the e-e interaction alone shifts the peak to higher energies[19] the strong renormalization of the electronic energies due to the presence of phonons in the system compensates this shift and produces an overall opposite effect.[17]

In support of the interpretation that the bistability is physically due to coexisting states with different charge in the space between the barriers[2,14,15,16] we show in Fig. 3 the charge density $\langle n_l \rangle$ at several values of the bias. We use arbitrary units. Here and below $W_c = 3W_e$. The charge in the well increases steadily with the voltage, and then drops abruptly when the threshold value $V_{\mathrm{th}}^{\uparrow}$ is reached. If, after going beyond this threshold, the bias is decreased [dashed line in the inset of Fig. 3(c)] no significant charge buildup is present up to a bias $V_{\mathrm{th}}^{\downarrow} < V_{\mathrm{th}}^{\uparrow}$, exhibiting the existence of a second stable solution in the region $V_{\mathrm{th}}^{\downarrow} < V < V_{\mathrm{th}}^{\uparrow}$. At the bias $V_{\mathrm{th}}^{\downarrow}$ the charge builds up again and the two solutions merge. The charge in the well increases the local potential, thus allowing the resonance to keep its alignment with the Fermi sea in the emitter. When the well is empty this effect is absent. The phonon peak is accompanied by a similar increase of charge in the well. It is much smaller, however, and only in the limit of strong asymmetry does it produce a bistable region.

In Fig. 4 we show results for finite values of the magnetic field. Notation is as in Fig. 2. The presence of a bistable region and a phonon peak is apparent in all cases. The main qualitative difference with the zero magnetic field results is the presence of structure in the curves. These plateaulike features are due to resonant levels in the space between the barriers, crossing the Fermi energy in the emitter. The magnetic field quantizes the motion in the transverse plane, forcing transport to take place between regions of one-dimensional character at either side of the sample, through a region of zero-dimensional character in the well space between the barriers. Each Landau level gives rise to a parabolic dispersion law in the emitter and collector regions, and a single resonant level in the well. These parabolas and iso-

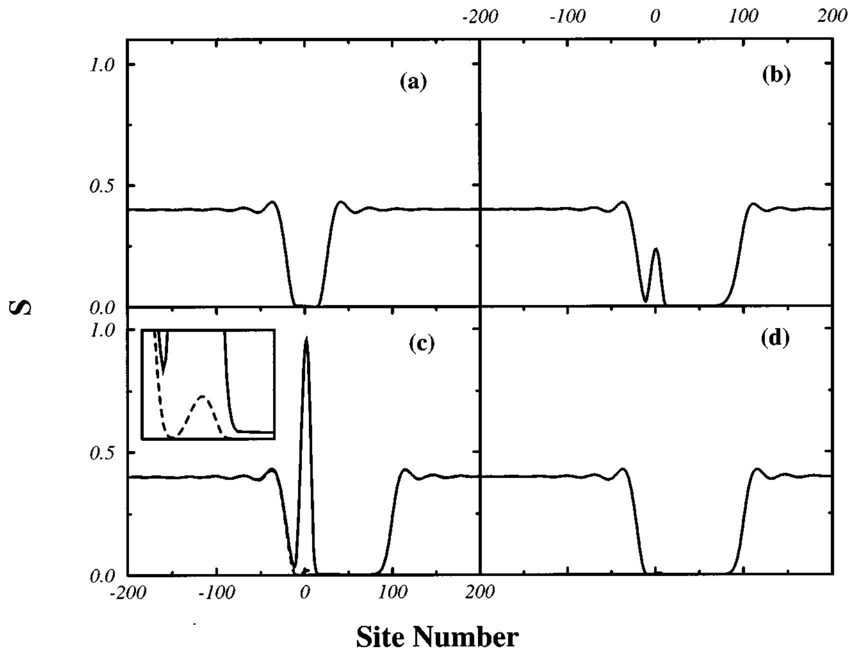

FIG. 3. Dimensionless charge density $\langle n_l \rangle$ at 0 T for (a) 0.02 V, (b) 0.05 V, (c) 0.21 V, and (d) 0.3 V.

lated resonances form ladders with the energy step $\hbar\omega_c$. As the bias is increased, the resonant energy levels in the well move down with respect to the Fermi energy, crossing it and thus opening a channel for transport, whenever the conservation of Landau index condition is fulfilled. Because the separation between levels scales with the magnetic field, the increase in bias necessary to open a new channel increases with the field also. This effect may be appreciated by comparing the various curves in the figure.

Another manifestation of the opening of new transport channels is the oscillation with magnetic field that is observed in the threshold voltage $V_{\rm th}^{\uparrow}$. This is shown in Fig. 5. At very high fields only the first Landau level is an open channel. As the field decreases new channels come into play one after the other, each entrance marked by a maximum in $V_{\rm th}^{\uparrow}$. These oscillations correspond to fluctuations of the Fermi energy, which in turn produce oscillations in the charge that gets trapped in the well region. Similar oscillations have been observed experimentally.[9] At very large magnetic fields, when only one Landau channel is open, we found instabilities in our self-consistent numerical calculations, probably due to an enhanced nonlinearity in the equations. The physical implications of these instabilities are currently under investigation.

V. SUMMARY

In summary, we have studied the transport through an asymmetric double barrier in the presence of a longitudinal magnetic field. We include both the electron-electron and

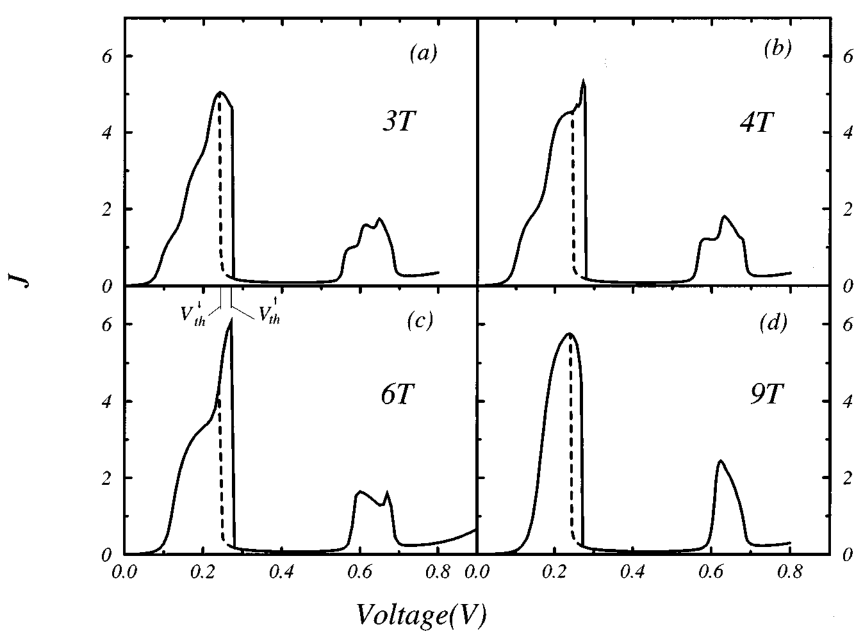

FIG. 4. Current-voltage characteristics for finite magnetic field. (a) $B=3$ T, (b) $B=4$ T, (c) $B=6$ T, and (d) $B=9$ T.

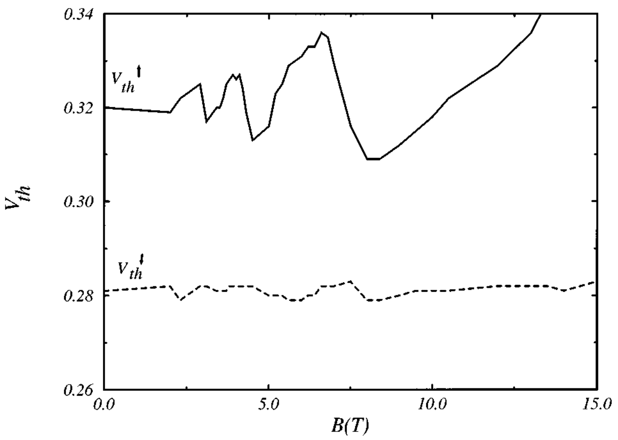

FIG. 5. Threshold voltage when increasing ($V_{\rm th}^{\uparrow}$) or decreasing ($V_{\rm th}^{\downarrow}$) the bias.

electron-phonon interactions. The first produces bistable regions in the I-V characteristics while the second opens an inelastic channel for resonant tunneling with the creation of phonons, giving rise to another peak in the current. In the bistable region two solutions coexist, one with a large charge density in the space between the barriers and a second with essentially no charge in that space. The width of this region depends on the ratio of the barrier thicknesses. It is absent when these are equal, and we predict that it saturates to a fixed finite value at $W_c \sim 6 W_e$. Also, the height of the main peak decreases as the collector barrier is increased, while the phonon peak remains essentially unchanged. We predict that in the limit of large asymmetry a bistable solution is also possible in the phonon peak.

The magnetic field produces oscillations in the current when the bias is changed at fixed field, and in the width of the bistable region at fixed bias when the magnetic field changes. Both these effects have been seen in experiment.[3,9] They are due to the peculiar density of states that arises from quantization of the motion perpendicular to the field. Each feature in the structure corresponds to a channel being opened or closed as the bias or magnetic field are changed.

ACKNOWLEDGMENTS

This work was supported in part by FONDECYT, Grants Nos. 1930553 and 3950026, CNPq, CLAF, Fundacio´n Andes/Vitae/Antorchas, and FINEP.

[1] L. Chang, L. Esaki, and R. Tsu, Appl. Phys. Lett. **24** , 593 (1974).

[2] V.J. Goldman, D.C. Tsui, and J.E. Cunningham, Phys. Rev. Lett. **58**, 1256 (1987).

[3] A. Zaslavsky, D.C. Tsui, M. Santos, and M. Shayegan, Phys. Rev. B **40**, 9829 (1989).

[4] V.J. Goldman, D.C. Tsui, and J.E. Cunningham, Phys. Rev. B **36**, 7635 (1987).

[5] N.S. Wingreen, K.W. Jacobsen, and J.W. Wilkins, Phys. Rev. B **40**, 11 834 (1985).

[6] E. Anda and F. Flores, J. Phys. Condens. Matter **3**, 9087 (1991).

[7] M. Jonson, Phys. Rev. B **39**, 5924 (1989).

[8] L. Eaves, M. L. Leadbeater, D.G. Hayes, E.S. Alves, F. W. Sheard, G. A. Toombs, P. E. Simmonds, M. S. Skolnick, M. Henini, and O. H. Hughes, Solid State Electron. **32**, 1101 (1989).

[9] M. L. Leadbeater and L. Eaves, Phys. Scr. **T35**, 215 (1991).

[10] N. Kamata, K. Yamada, N. Miura, and L. Eaves, Physica B **184**,250 (1993).

[11] P.J Turley, C.R. Wallis, S.W. Teitsworth, W. Li, and P.K. Bhattacharya, Phys. Rev. B **47**, 12 640 (1993).

[12] V.J. Goldman, D.C Tsui, and J.E. Cunningham, Phys. Rev. B **35**, 9387 (1987).

[13] E. Anda, S. Makler, H. Pastawski, and R. Barrera, Brazilian J. Phys. **24**, 330 (1994).

[14] F.W. Sheard and G. A. Toombs, Appl. Phys. Lett. **52**, 1408 (1988).

[15] P. Orellana, F. Claro, and E. Anda, Physica A **257**, 457 (1994).

[16] A. Zaslavsky, V. J. Goldman, D. C. Tsui, and J. E. Cunningham, Appl. Phys. Lett. **53**, 1408 (1988).

[17] G. Mahan, in *Many Particle Physics* (Plenum, New York, 1981), pp. 269–272.

[18] M. Cahay, M. McLennan, S. Datta, and M.S. Lundstrom, Appl. Phys. Lett. **50**, 612 (1987).